Theory and Applications of the Robust Cross-Coupled Control Design

Syh-Shiuh Yeh

Pau-Lo Hsu

Department of Electrical and Control Engineering, National Chiao Tung University, Hsinchu, 300 Taiwan
plhsu@cc.nctu.edu.tw

The cross-coupled control (CCC) has been recognized as an efficient motion controller that reduces contouring errors, but theoretical analysis of it is lacking, and there is no systematic design approach for obtaining a CCC system with guaranteed control performance. Consequently, the compensators C in CCC are commonly implemented in a PID structure and their contouring accuracy is usually degraded in real applications under different operating conditions. In an attempt to overcome the CCC design limitations described above, this paper introduces a robust CCC design based on a novel formulation: the contouring error transfer function (CETF), leading to an equivalent formulation as in the feedback control design problem. Then, methods in robust control design can be readily employed to achieve robust CCC with specified stability margins and guaranteed contouring performance. Furthermore, the proposed design has been verified as being internally stable. All provided experimental results indicate that the proposed robust CCC design consistently renders satisfactory contouring accuracy under different operating conditions.

I Introduction

In motion control, feedback controllers for multiple-axis systems are usually designed independently such that each axial servomechanism can track input commands accurately to reduce tracking errors. However, such control structures can not further reduce tracking or contouring errors because of inherent servo lag, stick friction, or backlash constraints. Zero phase error tracking control (ZPETC) was proposed by Tomizuka (1987) to reduce effectively tracking errors. To reduce contouring errors, Koren (1980) proposed the cross-coupled controller (CCC) which substantially improves the contouring accuracy of multiple-axis systems by applying position error adjustment to each axis. Moreover, other CCCs of various types have been reported since Koren's original publication to achieve desirable contouring performance. For example, adaptive CCC was proposed by Chuang and Liu (1991, 1992), optimal CCC design method was proposed by Kulkarni and Srinivasan (1989, 1990), and fuzzy logic controlled CCC was proposed by Koren and Jee (1995). In general, the structure of CCC includes (1) cross-coupling gains (C_x, C_y) and (2) a compensator C. Recently, a variable-gain CCC was proposed (Koren and Lo, 1991), in which the gains (C_x, C_y) are adjusted in real time according to the contour geometry to further improve contouring accuracy.

Variable-gain CCC control systems process different contouring commands as parameter-varying systems. Moreover, motion control systems are usually operated under varied external loading. Therefore, the main objective that enable the compensator C design in a CCC to cope with different operating conditions in practice are

(1) effective reduction of contouring errors under differing contour conditions and loading, and
(2) guaranteeing that the CCC system will be stable under different operating conditions.

To meet these requirements, the compensator C must be designed with sufficient stability and guaranteed contouring performance. However, available CCC controllers have not been systematically analyzed yet, and PID-type compensators C that do not guarantee stability and performance are commonly adopted.

This paper presents a robust CCC design method by introducing a novel formulation, the contouring error transfer function (CETF) that describes the dynamic relationship between contouring errors produced by coupled-control systems and those produced by uncoupled-control systems. By this formulation, the CCC design can be simply represented in a feedback control design problem. Thus, robustness theories and analysis of control design can be directly employed in CCC design to achieve desirable stability margins and performance. In this paper, we use the quantitative feedback theory (QFT) design algorithm (Horowitz and Sidi, 1972) to achieve robust CCC with specified 50 dB gain margin and 90 deg phase margin. Furthermore, analysis indicates that the present robust CCC design is internally stable. Under different commands and loading conditions, experimental results indicate that the present robust CCC design consistently renders satisfactory contouring accuracy.

II CCC System Contouring Errors

A two-axis cross-coupled motion-control system is represented in Fig. 1. This CCC motion-control system has three degrees of freedom, two position loop controllers (K_{px}, K_{py}) and a compensator C. Figure 1 can be further simplified, as shown in Fig. 2. In general, if the position loop proportional gains (K_{px}, K_{py}) are set too small, the system response becomes sluggish, however large gains setting may cause system oscillation. Practically, the damping ratio of each position feedback loop is expected to be larger than 0.707 to avoid oscillatory motion.

Variable Gains in CCC. In the variable-gain CCC design, the cross-coupling gains (C_x, C_y) are directly determined according to the contouring commands (Koren and Lo, 1991). For linear contours, the gains (C_x, C_y) are determined by

$$C_x = \sin\theta \tag{1}$$

$$C_y = \cos\theta \tag{2}$$

Contributed by the Dynamic Systems and Control Division for publication in the JOURNAL OF DYNAMIC SYSTEMS, MEASUREMENT, AND CONTROL. Manuscript received by the Dynamic Systems and Control Division October 7, 1996. Associate Technical Editor: Tsu-Chin Tsao.

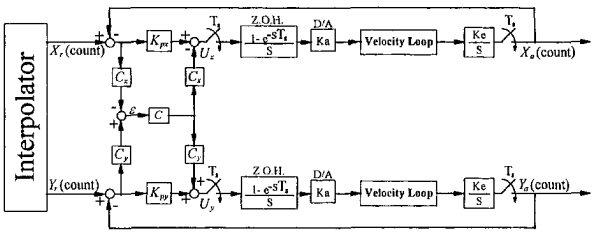

Fig. 1 Two-axis cross-coupled motion-control system

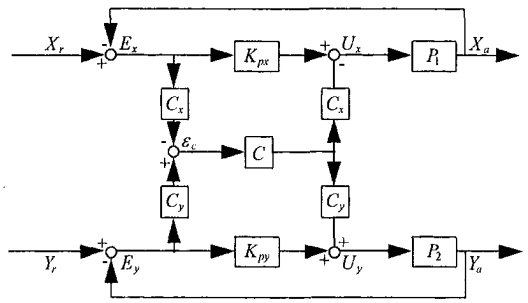

Fig. 2 Block diagram of the coupled motion-control system

where θ is the inclination angle of a linear contour with respect to X-axis. For circular contours, the variable gains (C_x, C_y) are determined by

$$C_x = \sin\theta - \frac{E_x}{2R} \tag{3}$$

$$C_y = \cos\theta + \frac{E_y}{2R} \tag{4}$$

where R is the circular contour radius, (E_x, E_y) are X-axis and Y-axis error signals, respectively; θ is the circular contour traversal angle input command. As shown in Eqs. (1)–(4), the cross-coupling gains are determined by the orientation in linear motions and by the traversal angle in circular motions. Therefore, the CCC control system which combines the CCC controller and the plant is a parameter-varying system. If the axial errors are much smaller than the circular motion circle radius (Koren and Lo, 1991), the cross-coupling gains (C_x, C_y) in Eqs. (1)–(4) can be reasonably confined in the range of $[-1, 1]$ in the CCC design. The template used for the QFT design algorithm can be thus constructed for further robust design.

Uncoupled Systems. To analyze an uncoupled system, let $C = 0$ and ε_o be the uncoupled motion-control system contouring error, where the subscript "o" represents the open cross-coupling connection. The corresponding variables shown in Fig. 2 are represented as

$$\varepsilon_o = E_yC_y - E_xC_x \tag{5}$$

$$U_x = K_{px}E_x; \quad U_y = K_{py}E_y \tag{6}$$

$$X_a = P_1U_x; \quad Y_a = P_2U_y \tag{7}$$

$$E_x = X_r - X_a; \quad E_y = Y_r - Y_a \tag{8}$$

From Eqs. (6)–(8), the axial errors (E_x, E_y) are

$$E_x = \frac{1}{1 + P_1K_{px}}X_r; \quad E_y = \frac{1}{1 + P_2K_{py}}Y_r \tag{9}$$

When Eq. (9) is substituted into Eq. (5), the contouring error of the uncoupled system becomes

$$\begin{aligned}\varepsilon_o &= E_yC_y - E_xC_x \\ &= \frac{C_y}{1 + P_2K_{py}}Y_r - \frac{C_x}{1 + P_1K_{px}}X_r \\ &= \frac{1}{(1 + P_2K_{py})(1 + P_1K_{px})} \\ &\quad \times [-(1 + P_2K_{py})C_x \ (1 + P_1K_{px})C_y]\begin{bmatrix}X_r \\ Y_r\end{bmatrix}\end{aligned} \tag{10}$$

Cross-Coupled Systems. Define ε_c as the contouring error of a coupled motion-control system, where the subscript "c" means "coupled system". As shown in Fig. 2, if $C \neq 0$ the variables are represented as

$$\varepsilon_c = E_yC_y - E_xC_x \tag{11}$$

$$U_x = K_{px}E_x - C\varepsilon_cC_x; \quad U_y = K_{py}E_y + C\varepsilon_cC_y \tag{12}$$

$$X_a = P_1U_x; \quad Y_a = P_2U_y \tag{13}$$

$$E_x = X_r - X_a; \quad E_y = Y_r - Y_a \tag{14}$$

From Eqs. (12)–(14), the axial errors (E_x, E_y) are

$$E_x = \frac{X_r + CC_xP_1\varepsilon_c}{1 + P_1K_{px}}; \quad E_y = \frac{Y_r - CC_yP_2\varepsilon_c}{1 + P_2K_{py}} \tag{15}$$

When Eq. (15) is substituted into Eq. (11), the contouring error of the coupled motion-control system ε_c becomes

$$\begin{aligned}\varepsilon_c &= E_yC_y - E_xC_x \\ &= \frac{C_yY_r - CC_yC_yP_2\varepsilon_c}{1 + P_2K_{py}} - \frac{C_xX_r + CC_xC_xP_1\varepsilon_c}{1 + P_1K_{px}} \\ &= \frac{1}{(1 + P_2K_{py})(1 + P_1K_{px})}\end{aligned}$$

Nomenclature

C = compensator in CCC
C_n, C_d = numerator and denumator of the compensator C
C_x, C_y = variable gains in CCC
E_x, E_y = position error of X and Y axes
GM, PM = gain margin and phase margin, respectively
Ka = D/A gain (2.442×10^{-3} V/pulse)
Ke = encoder gain (632.62 pules/rad)
K_{px}, K_{py} = proportional gain controllers for X and Y position loops
M_p, ω_p = the maximum gain M_p and corresponding frequency ω_p of contouring error transfer function T
P_1, P_2 = equivalent controlled plant of X and Y axes
T = contouring error transfer function
ε_c = contouring error of coupled motion control system
ε_o = contouring error of uncoupled motion control system
ω_o = reference frequency of template

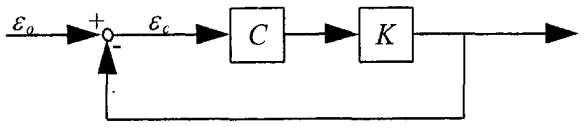

Fig. 3 An equivalent CCC control system

$$\times [(C_y Y_r - CC_y C_y P_2 \varepsilon_c)(1 + P_1 K_{px}) - (C_x X_r + CC_x C_x P_1 \varepsilon_c)(1 + P_2 K_{py})] \quad (16)$$

Eq. (16) can be rewritten as

$$[(1 + P_2 K_{py})(1 + P_1 K_{px}) + (1 + P_1 K_{px}) CC_y C_y P_2 + (1 + P_2 K_{py}) CC_x C_x P_1] \varepsilon_c = (1 + P_1 K_{px}) C_y Y_r - (1 + P_2 K_{py}) C_x X_r \quad (17)$$

Then, the contouring error ε_c can be represented as

$$\varepsilon_c = \frac{1}{[(1 + P_2 K_{py})(1 + P_1 K_{px}) + (1 + P_1 K_{px}) CC_y C_y P_2 + (1 + P_2 K_{py}) CC_x C_x P_1]} \cdot [-(1 + P_2 K_{py}) C_x \; (1 + P_1 K_{px}) C_y] \begin{bmatrix} X_r \\ Y_r \end{bmatrix} \quad (18)$$

III The Contouring Error Transfer Function

Using Eqs. (10) and (18), and introducing the following two representations

$$\alpha = (1 + K_{px} P_1)(1 + K_{py} P_2)$$

$$\beta = (1 + K_{px} P_1) CC_y C_y P_2 + (1 + K_{py} P_2) CC_x C_x P_1$$

the contouring error for the uncoupled and coupled systems can be simply represented as

$$\varepsilon_o = \frac{1}{\alpha} [-(1 + P_2 K_{py}) C_x \; (1 + P_1 K_{px}) C_y] \begin{bmatrix} X_r \\ Y_r \end{bmatrix} \quad (19)$$

$$\varepsilon_c = \frac{1}{\alpha + \beta} [-(1 + K_{py} P_2) C_x \; (1 + K_{px} P_1) C_y] \begin{bmatrix} X_r \\ Y_r \end{bmatrix} \quad (20)$$

respectively. By combining Eqs. (19)–(20), the relationship of the contouring error to the coupled and uncoupled systems can be derived as

$$\varepsilon_c = \frac{1}{1 + \dfrac{\beta}{\alpha}} \varepsilon_o = \frac{1}{1 + CK} \varepsilon_o = T \cdot \varepsilon_o \quad (21)$$

where C is the compensator in the CCC to be designed, and

$$K = \frac{(1 + K_{px} P_1) C_y C_y P_2 + (1 + K_{py} P_2) C_x C_x P_1}{(1 + K_{px} P_1)(1 + K_{py} P_2)} \quad (22)$$

$$T = \frac{1}{1 + CK} \quad (23)$$

As represented in Eqs. (21)–(23), the functional relationship T between the coupled and uncoupled motion-control systems is defined as the contouring error transfer function (CETF). When the cross-coupling gains are changing during a contour motion, both the K and T in Eq. (21) are parameter-varying functions.

An Equivalent CCC Design. Note that in Eqs. (21)–(23), the CETF is similar to the sensitivity function in a feedback control system. Therefore, the CETF can be further represented as an equivalent feedback control loop, as shown in Fig. 3. Consequently, the design goals of the compensator C in CCC become reduction of the contouring error ε_c, and stabilizing the equivalent CCC control system. Note that with the present CETF formulation, various robust algorithms for controller design can be directly employed to achieve desirable stability margins and performance. Moreover, the compensator C design in the present CCC for the two-axis servo system can be simplified to a single-loop design problem.

In CCC design, the relationship between the coupled system stability and the equivalent feedback control loop as shown in Fig. 3 is examined below.

Theorem 1 (Yeh, 1990)

For internally connected systems, the input signals are injected into each internal connection point to result in the mixed output signals. The internally connected systems are internally stable if the set of all input signals and output signals are bounded-input-bounded-output (BIBO) stable.

Theorem 2

If the CCC controlled system is designed to meet the following requirements:

(A1) the position feedback loop controller (K_{px}, K_{py}) achieves internal stability for each axis, and

(A2) the equivalent CCC control system, as shown in Fig. 3, remains internally stable as the cross-coupling gains (C_x, C_y) are changed,

then the designed coupled system as shown in Fig. 2 is internally stable.

Proof: We can prove this theorem for the CCC controlled system by examining the transfer functions between injected input signals and mixed output signals. Clearly, the requirements (A1) and (A2) achieve all stable zeros of the rational function $(\alpha + \beta)$, where α and β are both defined as previous. Since the poles of the rational function $(\alpha + \beta)$ contains the poles of the forward path gains between each injected bounded input signal and each mixed output signal, the poles of the transfer function for each injected bounded input signal and each mixed output signal in Fig. 2 are thus stable. Therefore, from Theorem 1, the coupled motion-control system is internally stable.

According to Theorem 2, the design requirement (A1) can be accomplished independently by designing a position loop feedback controller for each axis. By applying available robust design methods to the equivalent CCC control system, as shown in Fig. 3, the design requirement (A2) can be thus directly achieved.

Define $P_1 = P_{1n}/P_{1d}$, $P_2 = P_{2n}/P_{2d}$, and $C = C_n/C_d$, the rational function K can then be represented as

$$K = \frac{C_y^2 P_2 (1 + K_{px} P_1) + C_x^2 P_1 (1 + K_{py} P_2)}{(1 + K_{px} P_1)(1 + K_{py} P_2)} = \frac{C_y^2 P_{2n} (P_{1d} + K_{px} P_{1n}) + C_x^2 P_{1n} (P_{2d} + K_{py} P_{2n})}{(P_{1d} + K_{px} P_{1n})(P_{2d} + K_{py} P_{2n})}. \quad (24)$$

Since the uncoupled motion control system is internally stable, both the polynomial $(P_{1d} + K_{px} P_{1n})$ and $(P_{2d} + K_{py} P_{2n})$ have stable roots. In other words, the stable poles of the rational function K are fixed and independent of the cross-coupling gains.

IV Robust Design of Compensator C

Since the sampled data control system is usually a nonminimum phase system (Ogata, 1970; Astrom, 1984; Golten, 1991), the gain margin and phase margin are both larger than zero in discrete-time domain frequency analysis can not guarantee the stability of systems. Therefore, the general version of the Nyquist stability criterion for digital control (Kuo, 1992) is employed in the present design.

Because the CETF represented as $T = 1/(1 + CK)$ for the cross-coupled system is similar to the sensitivity function in the control design shown in Fig. 3, the four design requirements for a compensator C that produces satisfactory stability are as follows:

(B1) the robust compensator have only one pole at $z = 1$; i.e.,

$$C(z) = \frac{1}{(z - 1)} \hat{C}(z)$$

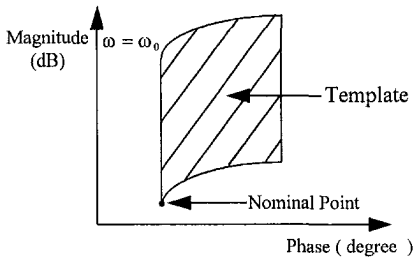

Fig. 4 The template at reference frequency $\omega = \omega_o$ (rad/s)

(B2) $\hat{C}(z)$ is the minimum phase rational function, and

(B3) the rational function $CK(z)$ is strictly proper, and has no real zeros equal to or larger than one.

(B4) the rational function $CK(z)$ has both positive gain and phase margins in frequency domain analysis.

According to the general version of Nyquist stability criterion, the robust compensator design to meet requirements (B1)–(B4) guarantee the equivalent CCC control system as shown in Fig. 3 to be internally stable as the cross-coupling gains are changed. Although the above requirements (B1)–(B4) for the present CCC design are quite conservative, they can achieve guaranteed stability margins and contouring performance under different operating conditions.

In this paper, we adopted the quantitive feedback theory (QFT) design algorithm (Horowitz and Sidi, 1972) to achieve a robust CCC design. Since the cross-coupling gains are changed for different contour motions, their variation range $[-1, 1]$ can be modeled as the uncertainty in the QFT design to achieve robust CCC systems. The design theory of the QFT algorithm is to move the template of the rational function $K(z)$ to meet design specifications by robust compensator $C(z)$ at certain reference frequencies. Thus, the rational function $CK(z)$ which achieves desired frequency responses provides sufficient stability margins under the different cross-coupling gains. The template can be constructed by varying the cross-coupling gains from -1 to 1, as shown in Fig. 4. In Eq. (21), the gain and the phase responses of the rational function $CK(z)$ can be represented as

$$|CK(e^{j\omega_o T_s})|_{\text{dB}} = |C(e^{j\omega_o T_s})|_{\text{dB}} + |K(e^{j\omega_o T_s})|_{\text{dB}} \quad (25)$$

$$\angle[CK(e^{j\omega_o T_s})]_{\text{degree}} = \angle[C(e^{j\omega_o T_s})]_{\text{degree}} + \angle[K(e^{j\omega_o T_s})]_{\text{degree}}, \quad (26)$$

The frequency response of $K(e^{j\omega_o T_s})$ is shifted by $(\angle[C(e^{j\omega_o T_s})]_{\text{degree}}, |C(e^{j\omega_o T_s})|_{\text{dB}})$ according to the compensator frequency response $C(e^{j\omega_o T_s})$ at the reference frequency $\omega = \omega_o$ (rad/sec), and the template of the rational function $K(z)$ is thus shifted according to the design of the robust compensator $C(z)$. Therefore, the present robust compensator C can be designed such that the frequency responses of the rational function CK at certain reference frequencies satisfy the design specifications.

In consideration of the gain response of the CETF, the QFT design algorithm can be represented on the inverse Nichol's Chart. Each point on the same curve on the inverse Nichol's Chart implies the same magnitude M of the transfer function T; i.e., $M = |T| = |1/(1 + CK)|$, and each point on the inverse Nichol's Chart is the magnitude and phase frequency responses of the rational function $CK(z)$. Thus, the template of the rational function $K(z)$ has to be moved into a suitable region by applying lead or lag compensators designed to keep the frequency response of the rational function $CK(z)$ within the specified gain margin, phase margin and suitable gain response of the CETF in order to maintain system stability and reduce contouring errors when the cross-coupling gains are changed.

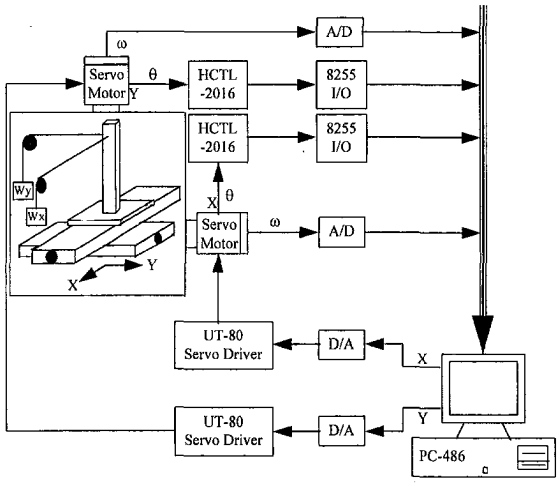

Fig. 5 The experimental setup

V Implementation of the Robust CCC

The experimental setup for the present study is shown in Fig. 5. The PC-486 generated the main control commands and recorded the signals including: the input command calculation for different contours, the implementation of a variable-gain CCC controller, and the control inputs to the velocity loop. The Sanyo UT-80 DC servo driver with analog current signal feedback included a velocity loop, a current loop, and a PWM output. The PC-486 interface utilized an AD/DA card to send and receive the control inputs and position outputs respectively at a sampling period of 1 ms.

The Position Loop. To identify the velocity loop for each axis, the axial control input was given a pseudo random binary sequence (PRBS) and the systems were modeled as the ARX model (Söderström, 1989). Then, the equivalent digitally controlled plants (P_1, P_2), as shown in Fig. 2, for the present biaxial motion-control system were obtained as

$$P_1(z^{-1}) = \frac{0.0026z^{-1} + 0.005z^{-2} + 0.0018z^{-3} + 0.0022z^{-4} - 0.0003z^{-5} + 0.0006z^{-6}}{1 - 1.5957z^{-1} + 0.5804z^{-2} - 0.322z^{-3} + 0.3099z^{-4} + 0.1701z^{-5} - 0.2070z^{-6} + 0.11z^{-7} - 0.0456z^{-8}} \quad (27)$$

$$P_2(z^{-1}) = \frac{0.0023z^{-1} + 0.0031z^{-2} + 0.0015z^{-3} - 0.0003z^{-4} - 0.0036z^{-5} + 0.0003z^{-6}}{1 - 1.5578z^{-1} + 0.3473z^{-2} - 0.1946z^{-3} + 0.3141z^{-4} + 0.1933z^{-5} - 0.102z^{-6} + 0.1997z^{-7} - 0.2001z^{-8}} \quad (28)$$

To achieve both stable motion and matched gains for the uncoupled two-axis system (Poo et al., 1972), the position loop proportional gains (K_{px}, K_{py}) were set at

$$K_{px} = 0.28$$

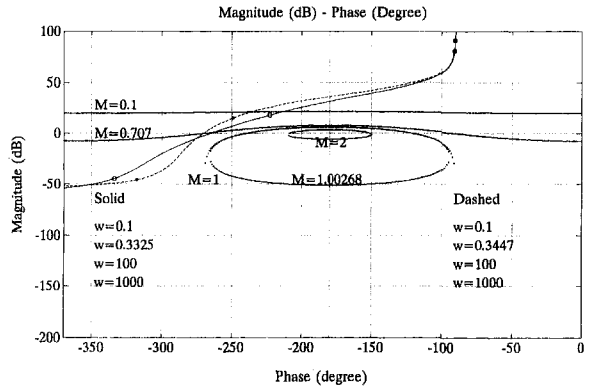

Fig. 6 The frequency response of the rational function $CK(z)$ with the integral compensator $C(z)$ (——: (C_{x1}, C_{y1}), · · · · · : (C_{x2}, C_{y2}))

$$K_{py} = 0.2544$$

Compensator C Design. To maintain system stability and achieve suitable CETF gain response, the conservative design specifications were set at a 50 dB gain margin, and a 90 deg phase margin. By applying the robust compensator design requirements (B1)–(B4) and the QFT design algorithm, the robust compensator was obtained as

$$C(z) = \frac{0.5z^4 - 1.4625z^3 + 1.4713z^2 - 0.5504z + 0.0417}{z^4 - 1.0450z^3 + 0.0457z^2 - 0.0007z + 3 \times 10^{-6}} \tag{29}$$

To examine the system stability and the gain response of the CETF for different compensators, the frequency response of the rational function $CK(z)$ with the digital integral compensator $C(z) = 1/(z - 1)$, a basic form in requirement B(1), was compared with the robustly designed compensator $C(z)$, as in Eq. (29). We considered two linear commends of 79.38 and 13.24 degrees, respectively. Their corresponding cross-coupling gains (C_{x1}, C_{y1}) and (C_{x2}, C_{y2}) were (0.9829, 0.1843) and (0.2290, 0.9734), respectively. The frequency responses of the rational function $CK(z)$ for different compensators, $C(z) = 1/(z - 1)$ and $C(z)$ as in Eq. (29), with different cross-coupling gains are shown in Fig. 6 and Fig. 7, respectively. As shown in Fig. 6, the frequency responses of the rational function $CK(z)$ with the digital integral compensator $C(z) = 1/(z - 1)$ have both negative gain margins and phase margins, the cross-coupled system is thus unstable. As shown in Fig. 7, the frequency performance of all gain and phase margins for these gain variations are positive. Furthermore, the designed results listed in Table 1 for the two different linear

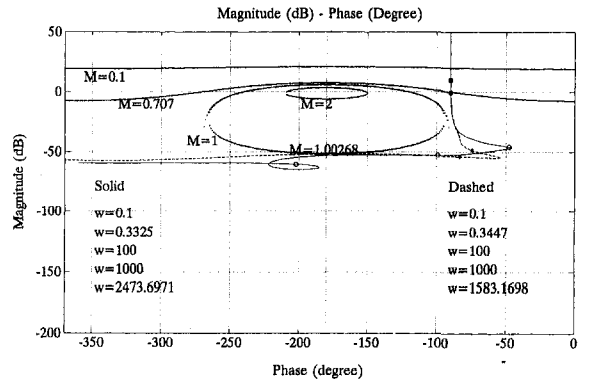

Fig. 7 The frequency response of the rational function $CK(z)$ with the robust compensator $C(z)$ (——: (C_{x1}, C_{y1}), · · · · · : (C_{x2}, C_{y2}))

Table 1 Frequency responses of the robust CCC design

Degree of the line	79.38	13.24
(C_x, C_y)	(0.9829, 0.1843)	(0.2290, 0.9734)
M_p	1.00232	1.00268
ω_p (rad/sec)	1682.1172	1583.1698
GM (dB)	51	50
PM (degree)	90	90

commands meet the frequency response specifications well. Moreover, the maximum gain of the CETF is only 1.00268 in the present CCC. Therefore, in addition to the guaranteed stability, the contouring error is also effectively suppressed by the present CCC design.

VI Experimental Results

Different Contouring Commands. Since the design of the robust CCC was based on linear contours, experiments were conducted involving three typical motion commands to verify its robustness:

(1) linear command: a linear command with 79.38 degree inclination angle, 20.3485 mm length at a speed of 1.2852 m/min for 0.95 seconds.

(2) corner command: a corner command is composited of two linear commands. The first linear segment of the corner command with 79.38 degree inclination angle, 20.3485 mm length at a speed of 1.2852 m/min for 0.95 seconds; the second linear command with 13.24 degree inclination angle, 21.8303 mm length at a speed of 1.31 m/min for 1 seconds.

(3) circular command: a circular command was performed with a 6.25 mm radius at a speed of 1.9635 m/min for 1.2 seconds.

We also compared the performance among three controllers, (1) an uncoupled controller with only a position loop controller **P,** (2) the proposed robust CCC, denoted as **CCC(robust),** and (3) a CCC in PID format, denoted as **CCC(PID).** We adopted the following parameters for the **CCC(PID),** Kp = 3.4, Ki = 6.2, and Kd = 0.11 which were obtained using the learning automata technique, specifically, under the circular command (Chen, 1995).

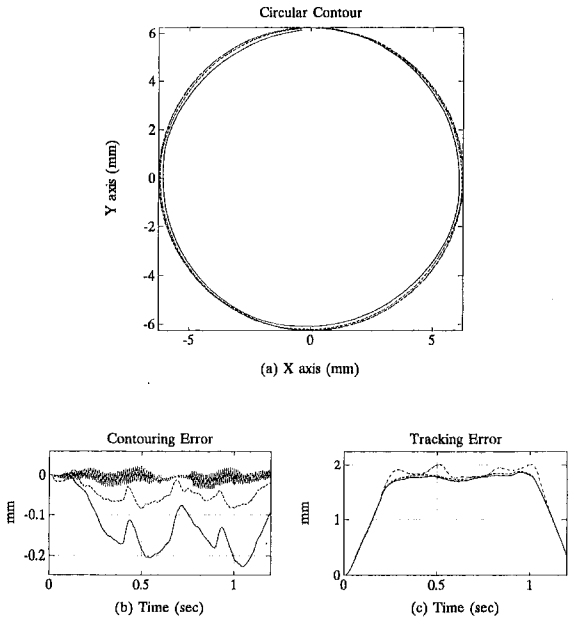

Fig. 8 Results for circular contouring. (a) Circular contour. (b) The corresponding contouring error. (c) The corresponding tracking error. (· · · · · : P + CCC(Robust), - · - · : P + CCC(PID), ——: P)

Table 2 Experimental measures of linear contouring

Error measure/controller	IAE (mm)	ISE (mm^2)
P	7.7592	0.1832
P + CCC(Robust)	3.1001	0.0433
P + CCC(PID)	10.6111	0.1548

Table 3 Experimental measures of corner contouring

Error measure/controller	IAE (mm)	ISE (mm^2)
P	59.4292	21.7336
P + CCC(Robust)	30.5961	12.6868
P + CCC(PID)	61.7025	16.6428

Table 4 Experimental measures of circular contouring

Error measure/controller	IAE (mm)	ISE (mm^2)
P	154.2828	24.9959
P + CCC(Robust)	54.8602	3.1295
P + CCC(PID)	11.1431	0.1637

Experimental results for the circular contouring command are shown in Fig. 8. Moreover, the normalized statistical results of corresponding integrals of absolute error (IAE) and integrals of square error (ISE), as listed in Tables 2–4, were also plotted, as shown in Fig. 9. Results indicate that compared with the uncoupled control system, the present robust CCC not only achieves significantly improved contouring accuracy, but also maintains the accuracy over all contouring commands presented. Note that the **CCC(PID),** which was specifically tuned for circular motion did achieve the least circular contouring error, as shown in Fig. 9. However, it became oscillation when applied to linear and corner contours, because an optimally tuned **CCC(PID)** is only marginally stable. As a whole, results indicate that the present robust CCC rendered the best contouring accuracy over all commands presented.

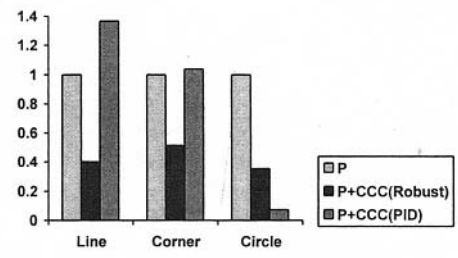

(a) IAE performance index

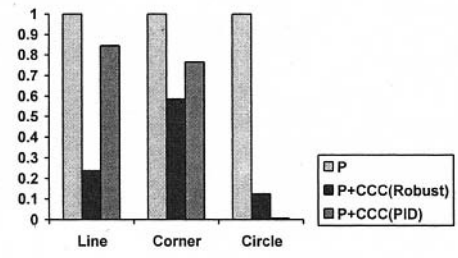

(b) ISE performance index

Fig. 9 Contouring errors for different compensators

Table 5 Performance measures under loading for corner contouring

Loading	No load		30 kg weight on each axis	
Error measure/ controller	IAE (mm)	ISE (mm^2)	IAE (mm)	ISE (mm^2)
P	59.4292	21.7336	67.7116	24.1695
P + CCC(Robust)	30.5961	12.6868	38.8027	13.9260

Table 6 Performance measures under loading for circular contouring

Loading	No load		30 kg weight on each axis	
Error measure/ controller	IAE (mm)	ISE (mm^2)	IAE (mm)	ISE (mm^2)
P	154.2828	24.9959	190.4763	45.1249
P + CCC(Robust)	54.8602	3.1295	61.7682	5.0257

Loading Conditions. In practice, motion-control systems are operated under either known or unknown loading conditions. Therefore, the present robust CCC design was also tested under a loading condition of 30 kg on each servo axis. The normalized statistical results for IAE and ISE for the corner and circular contours under loading, as listed in Tables 5–6. Results indicate that apparently, loading increased contouring errors in all cases. Nevertheless, the motion accuracy for the robust CCC still remained well even under different commands, as shown in Fig. 9. Clearly, the present design with sufficient stability margins makes the proposed robust CCC widely applicable.

VII Conclusions

This paper presents the theory and applications of a robust CCC design for motion-control systems. Based on a novel formulation of CETF, the design of the compensator C in the CCC is simply equivalent to a feedback-control design problem. Thus, available robust control theories can be applied to the proposed robust CCC design to achieve sufficient stability and contouring performance. For the present two-axis motion-control system, the CCC design is simplified to an SISO system and the QFT control design algorithm is directly employed to obtain satisfactory stability and guaranteed performance.

Experimental results indicate that the present robust CCC design achieves satisfactory contouring accuracy under different contouring commands and loading conditions. Although the robust CCC was designed with a fourth-order compensator in this case, the results provided by personal computer implementation have proven the feasibility of the present design.

References

Astrom, K. J., Hagander, P., and Sternby, J., 1984, "Zeros of Sampled Systems," *Automatica,* Vol. 20, pp. 31–38.

Chen, F. I., 1995, "Applications of the Learning Automata Method in Motion Control," Master thesis, Institute of Control Engineering, NCTU.

Chuang, H. Y., and Liu, C. H., 1992, "A Model Reference Adaptive Control Strategy for Improving Contour Accuracy of Multiaxis Machine Tools," *IEEE Trans. on Industry Application,* Vol. 28, No. 1, pp. 221–227.

Chuang, H. Y., and Liu, C. H., 1991, "Cross-Coupled Adaptive Feedrate Control for Multiaxis Machine Tools," ASME JOURNAL OF DYNAMIC SYSTEMS, MEASUREMENT, AND CONTROL, Vol. 113, No. 3, pp. 451–457.

Golten, J., and Verwer, A., 1991, *Control System Design and Simulation,* McGraw-Hill.

Horowitz, I. M., and Sidi, M., 1972, "Synthesis of Feedback Systems with Large Plant Ignorance for Prescribed Time-Domain Tolerance," *INT. J. Control,* Vol. 16, No. 2, pp. 287–309.

Hsu, P. L., and Houng, Y. C., 1996, "An Integrated Controller Design for Precise

CNC Motion Control," *CIRP Proceedings-Manufacturing Systems,* Vol. 25, No. 1, pp. 91–96.

Koren, Y., 1980, "Cross-Coupled Biaxial Computer for Manufacturing Systems," ASME JOURNAL OF DYNAMIC SYSTEMS, MEASUREMENT, AND CONTROL, Vol. 102, No. 4, pp. 265–272.

Koren, Y., and Lo, C. C., 1991, "Variable Gain Cross Coupling Controller for Contouring," *Annals of the CIRP,* Vol. 40, pp. 371–374.

Koren, Y., and Jee, S., 1995, "Fuzzy Logic Cross-Coupling Control," *CIRP Proceedings-Manufacturing Systems,* Vol. 25, No. 1, pp. 104–108.

Kulkarni, P. K., and Srinivasan, K., 1989, "Optimal Contouring Control of Multiaxis Drive Servomechanisms," ASME JOURNAL OF DYNAMIC SYSTEMS, MEASUREMENT, AND CONTROL, Vol. 111, No. 2, pp. 140–148.

Kulkarni, P. K., and Srinivasan, K., 1990, "Cross-Coupled Control of Biaxial Feed Drive Servomechanisms," ASME JOURNAL OF DYNAMIC SYSTEMS, MEASUREMENT, AND CONTROL, Vol. 112, No. 2, pp. 225–232.

Kuo, B. C., 1992, *Digital Control System,* Saunders HBJ.

Ogata, K., 1970, *Modern Control Engineering,* Prentice Hall.

Poo, A., Bollinger, J. G., and Younkin, W., 1972, "Dynamic Error in Type Contouring Systems," *IEEE Trans. on Industry Application,* Vol. IA-8, No. 4, pp. 477–484.

Söderström, T., and Stoica, P., 1989, *System Identification,* Prentice Hall.

Tomizuka, M., 1987, "Zero Phase Error Tracking Algorithm for Digital Control," ASME JOURNAL OF DYNAMIC SYSTEMS, MEASUREMENT, AND CONTROL, Vol. 109, pp. 65–68.

Yeh, F. B., 1990, *Post Modern Control Theory and Design,* Eurasia Book Company.